2004

A role for Tbx5 in proepicardial cell migration during cardiogenesis

Cathy J. Hatcher
Philadelphia College of Osteopathic Medicine, cathyha@pcom.edu

Nata Diman

Minsu Kim

David Pennisi

Yan Song

See next page for additional authors

Authors
Cathy J. Hatcher, Nata Diman, Minsu Kim, David Pennisi, Yan Song, Marsha M. Goldstien, Takashi Mikawa, and Craig T. Basson

A role for Tbx5 in proepicardial cell migration during cardiogenesis

Cathy J. Hatcher, Nata Y.S.-G. Diman, Min-Su Kim, David Pennisi, Yan Song, Marsha M. Goldstein, Takashi Mikawa and Craig T. Basson

Physiol. Genomics 18:129-140, 2004. First published 11 May 2004;
doi:10.1152/physiolgenomics.00060.2004

Physiological Genomics publishes results of a wide variety of studies from human and from informative model systems with techniques linking genes and pathways to physiology, from prokaryotes to eukaryotes. It is published quarterly in January, April, July, and October by the American Physiological Society, 9650 Rockville Pike, Bethesda MD 20814-3991. ISSN: 1094-8341, ESSN: 1531-2267. Visit our website at http://www.the-aps.org/.

Physiol Genomics 18: 129–140, 2004.
First published May 11, 2004; 10.1152/physiolgenomics.00060.2004.

TRANSLATIONAL PHYSIOLOGY

A role for Tbx5 in proepicardial cell migration during cardiogenesis

Cathy J. Hatcher,[1,2]* Nata Y. S.-G. Diman,[1,2]* Min-Su Kim,[1,2]* David Pennisi,[2] Yan Song,[1,2] Marsha M. Goldstein,[3] Takashi Mikawa,[2] and Craig T. Basson[1,2]

[1]*Molecular Cardiology Laboratory, Greenberg Cardiology Division, Department of Medicine, and* [2]*Department of Cell and Developmental Biology, Weill Medical College of Cornell University, New York, New York 10021; and* [3]*BioReference Laboratories, Elmwod Park, New Jersey 07407*

Submitted 5 March 2004; accepted in final form 7 May 2004

Hatcher, Cathy J., Nata Y. S.-G. Diman, Min-Su Kim, David Pennisi, Yan Song, Marsha M. Goldstein, Takashi Mikawa, and Craig T. Basson. A role for Tbx5 in proepicardial cell migration during cardiogenesis. *Physiol Genomics* 18: 129–140, 2004. First published May 11, 2004; 10.1152/physiolgenomics.00060.2004.— Transcriptional regulatory cascades during epicardial and coronary vascular development from proepicardial progenitor cells remain to be defined. We have used immunohistochemistry of human embryonic tissues to demonstrate that the TBX5 transcription factor is expressed not only in the myocardium, but also throughout the embryonic epicardium and coronary vasculature. TBX5 is not expressed in other human fetal vascular beds. Furthermore, immunohistochemical analyses of human embryonic tissues reveals that unlike their epicardial counterparts, delaminating epicardial-derived cells do not express TBX5 as they migrate through the subepicardium before undergoing epithelial-mesenchymal transformation required for coronary vasculogenesis. In the chick, *Tbx5* is expressed in the embryonic proepicardial organ (PEO), which is composed of the epicardial and coronary vascular progenitor cells. Retrovirus-mediated overexpression of human TBX5 inhibits cell incorporation of infected proepicardial cells into the nascent chick epicardium and coronary vasculature. TBX5 overexpression as well as antisense-mediated knockdown of chick Tbx5 produce a cell-autonomous defect in the PEO that prevents proepicardial cell migration. Thus, both increasing and decreasing Tbx5 dosage impairs development of the proepicardium. Culture of explanted PEOs demonstrates that untreated chick proepicardial cells downregulate Tbx5 expression during cell migration. Therefore, we propose that Tbx5 participates in regulation of proepicardial cell migration, a critical event in the establishment of the epicardium and coronary vasculature.

vasculature; epicardium; cardiac development

T-BOX TRANSCRIPTION FACTORS play critical roles in cardiovascular development. Mutations in the human *TBX5* gene cause abnormal cardiac morphogenesis in the context of autosomal dominant Holt-Oram syndrome (3, 32). Investigation of altered *Tbx5* gene dosage in several animal models has demonstrated defects in cardiac septation and myocardial growth and development similar to those observed in human individuals with Holt-Oram syndrome (6, 10, 23, 34). Normal cardiogenesis may reflect local myocardial balances between expression of T-box genes (57). Recent studies have also implicated T-box transcription factors in establishment of vascular structure. Murine studies demonstrated a role for Tbx1 in aortic arch development, and loss of human TBX1 may contribute to congenital cardiovascular abnormalities in patients with DiGeorge syndrome who have chromosome 22q deletions encompassing the *TBX1* gene (19, 27, 36, 46). The zebrafish T-box gene *hrT*, a homolog of chick and mouse *Tbx20*, is not only required for normal myocardial development and cardiac looping, but also for formation of the dorsal aorta (25, 28, 29, 45, 66). Expression analyses suggest a potential role for *Tbx18* in epicardial and vascular development, since this gene is highly expressed in the proepicardial organ (PEO) and the epicardium (28); both of these structures contribute to coronary vasculogenesis.

The PEO, a grape-like cluster of vesicles, comprises a discrete organ in the chick and a portion of the septum transversum in mammals. In the chick, the PEO initially forms as an outgrowth of the dorsal wall of the intra-embryonic coelom adjacent to the developing liver and becomes visible at the sinoatrial pole of the heart at Hamburger-Hamilton (HH) stage 13 (21). Each vesicle of the PEO is composed of multiple mesothelial cells, surrounding a fluid-filled lumen. By HH stage 18, the PEO contacts myocardium via villous projections forming tissue bridges. Proepicardial cells subsequently migrate over the myocardium to form the pericardium and the epicardial monolayer (42). Between HH stages 19–23, some epithelial cells migrate out of this layer into the subepicardial matrix and nascent myocardium. These cells undergo an epithelial-to-mesenchymal cell transformation (EMT) that contributes both to valvulogenesis in the endocardial cushions (18) and to differentiation of cardiac fibroblasts, endothelial cells, and coronary smooth muscle cells, all of which can participate in formation of the coronary vasculature (49).

Genetic cues originating in the myocardium are presumed to regulate the differentiation and localization of the epicardial mesenchyme and coronary blood vessels. Several genes, including the transcription factors *Tbx18* (28), *Gata4* (53), and *Fog2* (12, 65, 69), are expressed in the epicardium and coronary vasculature, but the molecular pathways that initiate and propagate epicardial EMT and coronary vasculogenesis remain to be delineated. Data suggest fine regulation of a balance among growth factors such as FGF and TGFβ isoforms as well as VEGF. Cell-cell and cell-matrix interactions are required, since this process requires connexin-43, VCAM-1, and α4-integrins (31, 33, 73). In addition, endothelin-mediated com-

*C. J. Hatcher, N. Y. S.-G. Diman, and M.-S. Kim contributed equally to this work.

Article published online before print. See web site for date of publication (http://physiolgenomics.physiology.org).

Address for reprint requests and other correspondence: C. T. Basson, Greenberg Cardiology Division, Dept. of Medicine, Weill Medical College of Cornell Univ., 525 E. 68th St., New York, NY 10021 (E-mail: ctbasson@med.cornell.edu).

munication between epicardial-derived cells (EPDCs) and primitive cardiomyocytes contributes to Purkinje fiber development (67). Transcriptional regulation during epicardial EMT involves WT-1, Ets transcription factors, and probably GATA transcription factors, whose roles are suggested by a requirement for Fog2 (12, 63, 69). A functional role for T-box transcription factors in epicardial EMT and coronary vasculogenesis has not yet been defined.

In this study, we demonstrate that human TBX5 is expressed in the coronary vasculature during embryogenesis and that variations in human TBX5 expression during cardiac morphogenesis correlate with activation of EPDC migration. We further analyzed the contribution of Tbx5 to proepicardial cell activity during chick cardiogenesis. Chick *Tbx5* is expressed in the PEO, and overexpression of human TBX5 inhibits cell migration out of the PEO and thereby impairs proepicardial cell contribution to the coronary vasculature. Proepicardial cell migration is altered by other perturbations in Tbx5 dosage, since antisense-mediated inhibition of Tbx5 translation also inhibits proepicardial cell migration. Notably, however, non-genetically engineered proepicardial cells repress Tbx5 expression during cell migration. Therefore, we propose that TBX5 can contribute to embryonic events that regulate proepicardial cell migration and thereby impact upon epicardial and coronary vascular development.

MATERIALS AND METHODS

Retroviral TBX5 constructs and infection of chick embryos in ovo. The CXIZ retrovirus and construction of the derivative wt-TBX5-CXIZ and Gly80Arg-TBX5-CXIZ replication-defective retroviruses, encoding wild-type and mutant TBX5 isoforms, respectively, have been previously described (23). Replication-defective viruses were propagated and titers were assayed per published protocols (23, 47, 67, 71). Ten to 100 viral particles in <10 nl containing 100 μg/ml Polybrene were pressure-injected in ovo into the PEO. PEO pressure injection was usually associated with a small amount of leakage of retrovirus into the adjacent myocardium. Eggs were resealed with Parafilm, and the embryos were maintained at 38°C until euthanasia. Euthanized embryos were fixed with 4% paraformaldehyde and stained overnight for β-galactosidase activity with X-Gal.

PEO explant, transfection, and cell culture. PEOs were microdissected from embryonic chicks at HH stages 16–18 prior to migration of the PEO over the myocardium. They were carefully trimmed to ensure the absence of any possible contaminating myocardium. Explanted PEOs were maintained in culture at 37°C, 5% CO_2 with DMEM media supplemented with 10% fetal bovine serum (FBS) and 2% chick serum for ≤72 h. For experiments involving overexpression of human TBX5, isolated PEOs were either infected with retrovirus or transfected with pEGFP-C1-TBX5 plasmid (11) or pEGFP-C1-TBX20 plasmid. To construct pEGFP-C1-TBX20 plasmid, human TBX20 1,287-bp cDNA was reverse transcribed (OneStep RT-PCR; Qiagen) from archived 14 wk human fetal heart (22) with primer hTBX20F (5′-ATTA**GAATTC**ATGCTGTTCTTTCCAGATCTTT-CCTTG-3′) and hTBX20R (5′-TAAT**TCTAGA**TCATACAAATG-GCGTCATCACAG-3′) and cloned into the *Eco*RI and *Xba*I restriction enzyme sites (shown in bold) in pEGFP-C1 plasmid (Clontech). Integrity of all constructs was confirmed by automated sequencing on an ABI 3100 (Applied Biosystems).

For retroviral infections, isolated PEOs were infected for 24 h with $>1 \times 10^6$ virions of CXIZ-derived retroviruses in the presence of 10 μg/ml Polybrene followed by continued culture for a further 48 h in virus-free media. For the plasmid transfections, PEOs were isolated, allowed to attach to the cell culture dish for 4 h, then transiently transfected with either pEGFP-C1, pEGFP-C1-TBX5, or pEGFP-C1-TBX20 in Opti-MEM media (GIBCO) using Lipofectamine Plus reagent per the manufacturer's instructions (Invitrogen). The cells were loaded 24 h later with Hoechst 33362 according to manufacturer's protocols (Sigma) and visualized by fluorescence microscopy (Nikon Diaphot 200) using SpotFinder software.

To study the consequences of gene knockdown, isolated PEOs were cultured in 12-mm wells and transfected with morpholino (MO) antisense oligomers for cTbx5, cTbx20, or the corresponding inverted (INV) sequences of each morpholino, as follows: cTbx5-MO (5′-GCCTTCCTCGGTGTCCGCCATGTTA-3′), cTbx20-MO (5′-CGGTGTGTACTCCATGGCGAGCCCC-3′), cTbx5-INV (5′-ATTGTACCGCCTGTGGCTCCTTCCG-3′), or cTbx20-INV (5′-CCCCGAGCGGTACCTCATGTGTGGC-3′) Each oligomer was covalently labeled with Lissamine (sulforhodamine B) fluorescent dye and synthesized to be used with the "Special Delivery" ethoxylated polyethylamine (EPEI) system (Gene Tools). The cTbx5-MO and cTbx20-MO sequences were designed to include sequence (−4 to +21 and −10 to +15) flanking the cTbx5 and cTbx20 translational start sites, respectively. Morpholino-modified antisense oligomers were transfected into PEOs according to the manufacturer's protocols and as previously described (51). Fluorescent microscopy of cultures permitted identification of transfected cells. After 3 h, transfection media was changed to fresh DMEM growth media.

Number of cells migrating out of PEOs after 24, 48, and 72 h of culture were determined by direct visualization with light microscopy. β-Galactosidase staining marked retrovirus-infected cells, and Lissamine fluorescence marked antisense oligomer transfected cells. For antisense studies, distribution of PEO cells was determined as the number of cells within 200-μm concentric rings surrounding the residual PEO explant. Statistical comparisons were made by ANOVA analysis with GB-STAT software.

Primary cultures of PEO cells were prepared using the previously described protocol for embryonic heart dispersion (30), with the exception of only one 15-min digestion with 0.5 mg/ml type II collagenase at 37°C (Worthington). To assess proliferation rates of retrovirus-infected cultured PEO cells, PEO cells were allowed to adhere to the culture surface for 3 h. For some studies, they were infected for 8 h with retroviruses and then grown for a further 13-h period in virus-free media. For other studies, cultured proepicardial cells were transfected with morpholino-modified antisense oligomers as described above. Twenty-four hours after plating collagenase-digested PEO cells, cultures either were used for RNA preparation or were fixed in 4% paraformaldehyde and underwent immunohistochemical staining with anti-β-galactosidase (ICN) and anti-PCNA (DAKO) antibodies using the LSAB2 kit with the EnVision Doublestain System (DAKO) per the manufacturer's instructions and as previously described (23). The fraction of PCNA-positive retrovirus-infected cells (marked by β-galactosidase positivity) was determined by direct visualization under light microscopy in triplicate samples. Statistical comparisons were made by ANOVA analysis with GB-STAT software.

RT-PCR of isolated PEO. Total RNA was isolated from either whole hearts or PEOs of HH stage 16–18 chicks with TRIzol per the instructions of the manufacturer (Invitrogen). In some cases, the explanted PEOs were maintained in culture for 72 h during which time some proepicardial cells migrated out of the explant. The initial PEO explant was detached from the dish and removed, leaving surrounding migrating PEO-derived cells. These PEO-derived cells were trypsinized, pelleted by centrifugation, and total RNA was isolated from them as well as from the removed PEO explant. RT-PCR for chick Tbx5 was performed on both populations of cells. To analyze chick Tbx5 mRNA expression by RT-PCR, 500 ng RNA were reverse transcribed and subsequently amplified by the OneStep RT-PCR kit (Qiagen) under the following conditions: 95°C for 30 s, 55°C for 45 s, 72°C for 1 min, for 30 cycles; followed by 72°C for 10 min. The primers used to amplify this 887-bp product were as follows:

cTbx5F (5′-CTGTGGCTGAAATTTCACGAGGTG-3′) and cTbx5R (5′-GGTAACTGGACCTGTACAAAGGAT-3′). Chick *GAPDH* mRNA expression was also analyzed in the same cell populations using primers 5′-ATGATTCTACACACGGACACTTCA-3′ and 5′-CTCATTGTCATACCAGGAAACAAG-3′. PCR products were analyzed on 2% agarose gels.

Quantitative RT-PCR. Quantitative RT-PCR was performed to assess expression levels of candidate chick genes in primary proepicardial cell cultures. Total RNA was isolated from cultures with TRIzol (Invitrogen), and cDNA was prepared from 1 μg of total RNA with the iScript cDNA synthesis kit (Bio-Rad). This cDNA served as template for real-time PCR studies using the Quantitech SYBR Green kit (Qiagen) and a Cepheid Smart Cycler. Reaction conditions were 95°C for 15 min and then 95°C for 30 s, 55°C for 30 s, and 72°C for 30 s, for 45 cycles. Genes analyzed and primers used were c*GAPDH* (5′-TGGGTGTCAACCATGAGAAATATG-3′; 5′-ACCTCTGTCATCTCTCCACAGCTT-3′), c*Tbx18* (5′-GTGCGCTGTACGGATATAACTTTT-3′; 5′-CTAAGTAAGTGCACTCCTTCCACA-3′), and c*Tbx20* (5′-AATTCGTTGAGAAGTCCTCCTG-3′; 5′-CAGGAGATTTTGGCCATCTCC-3′). Primer pairs were tested in standard PCR and shown to amplify a single product by agarose gel electrophoresis prior to use in real-time PCR assays. All real-time PCR reactions were matched with non-reverse-transcribed control reactions. Data from six replicate cultures were analyzed per published protocols (13).

In vitro isolated cell migration assays. Cell migration was measured using a quantitative assay of sheet migration as previously described (4, 5, 58) that was modified. Briefly, 1.25×10^6 D17 canine osteosarcoma cells were infected for 48 h with 10^7 virions of CXIZ-derived retrovirus in the presence of 10 μg/ml of Polybrene. Type I collagen-coated dishes were prepared as previously described (58). Retrovirus-infected D17 cells were trypsinized and resuspended in DMEM with 7% FBS to which 10 mM hydroxyurea was added to inhibit cell proliferation. One million cells were plated into the 10-cm central circular core of a 32-cm stainless steel circular fence (Yale Department of Biomedical Engineering) placed in a type I collagen-coated dish. After the cells attached to the dish overnight, the fence was removed. The cells were gently washed with PBS and allowed to migrate radially in culture media containing hydroxyurea. After migrating for 10 days, β-galactosidase-positive cells were visualized as previously described (23). Dishes were imaged on a flatbed scanner, and the diameter of the migrated cells was outlined and measured (Multi-Analyst software, Bio-Rad). The migration area was calculated as the diameter of cells after 10 days of migration minus the diameter of cells immediately following removal of the fence prior to the beginning of the migration assay. This value was expressed as square millimeters. Samples were analyzed in 25–30 replicate dishes, and statistical comparisons were made by ANOVA with GB-STAT software.

RNA probes and in situ hybridization. cDNA of *cTbx5* was synthesized from HH stage 16–18 chick heart RNA by RT-PCR using the previously named primer pair, cTbx5F and cTbx5R. The PCR product was TA-cloned into the pCRII vector (Invitrogen) and sequenced in both directions. Sense and antisense digoxigenin-labeled RNA probes were transcribed from *Xho*I and *Spe*I linearized plasmids, respectively, according to the manufacturer's instructions (Roche). Whole mount in situ hybridization on HH stage 16–18 chick embryos was performed as previously described (67). Following color development, embryos were paraffin embedded and sectioned at 10 μm as previously described (48).

Immunohistochemistry of human tissue. Human cardiac tissue was obtained as waste surgical pathology material from therapeutic abortions of 10 embryos at 10–15 wk gestation, with informed consent and approval of the Cornell Committee on Human Rights on Research, and tissues were prepared for immunohistochemistry as previously described (22). TBX5 protein was detected on 5-μm sections, which were analyzed and imaged on a Nikon Microphot microscope.

RESULTS

TBX5 expression in the human epicardium and coronary vasculature and in the chick PEO. Human embryonic tissue (10–15 wk of gestation) was analyzed by immunohistochemistry for TBX5 expression (Fig. 1) with a previously characterized (22) antibody to TBX5 that is directed against a specific TBX5 sequence carboxyl to the TBX5 T-box. In addition to

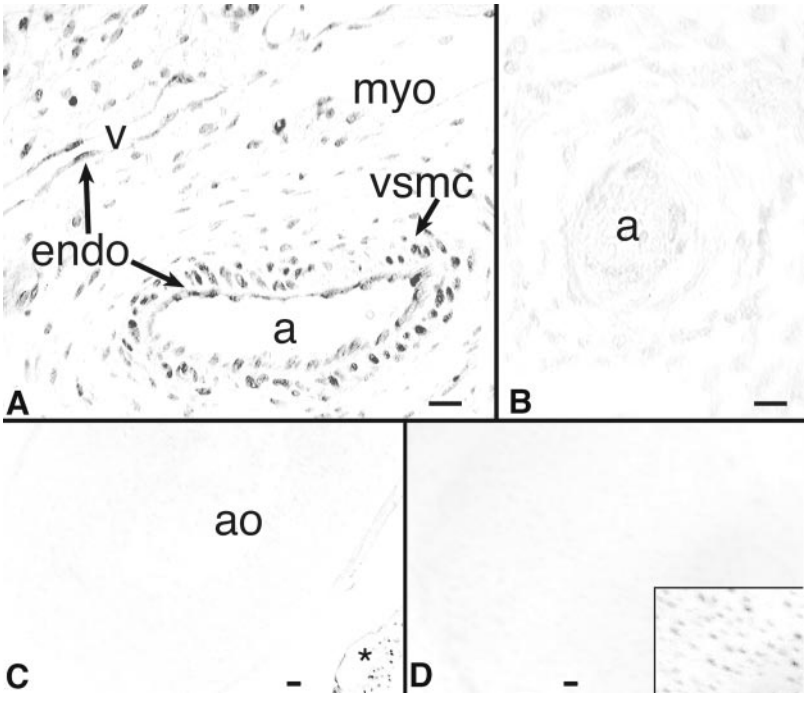

Fig. 1. Immunohistochemical detection of TBX5 in human embryonic heart and lung. Immunostaining for TBX5 in 15 wk of gestation human embryonic left ventricle (*A*) and lung (*B*). *A*: in the embryonic heart, TBX5 is expressed not only in the myocardium, but also in the smooth muscle and endothelial cells of coronary arteries (a) and veins (v). Vascular endothelial (endo) and smooth muscle (vsmc) cells are indicated as well as myocardial cardiomyocytes (myo). *B*: in the embryonic lung, no staining is seen in the vasculature; pulmonary arteriole is shown (a). *C*: no staining is observed in the aorta (ao) and the nascent outflow tract, although staining is observed in adjacent atrial myocardium (*). *D*: no staining is observed in the distal phalanx of the great toe despite staining of osteoblasts in the thumb (*inset*) costained in the same paraffin section. Bars = 20 μm.

previously described (22) expression in cardiomyocytes and atrioventricular nodal cells, marked staining for TBX5 was observed in the epicardium and coronary vasculature. TBX5 expression was observed in the coronary arterial and venous endothelium as well as in coronary arterial smooth muscle cells (Fig. 1*A*). TBX5 expression was not evident in vascular cells outside of the heart (Fig. 1, *B* and *C*), i.e., aorta, pulmonary artery, lungs, liver, kidney, and skeletal muscle. Absence of staining with the antibody used in the developing aorta (Fig. 1*C*) and foot (Fig. 1*D*), where TBX20 and TBX18, respectively, are known to be expressed (28, 29, 45), confirmed that the anti-TBX5 antibody used does not cross-react with these other T-box genes that are expressed in some vascular cells. As demonstrated previously, specificity of the antibody was verified by reacting tissue sections with anti-TBX5 antibody preadsorbed with the TBX5 peptide immunogen; no staining was observed in these sections (data not shown) (22).

Further analyses of human embryonic tissues also suggested EPDC inactivation of TBX5 expression in association with cell migration. During cardiogenesis, a subpopulation of EPDCs migrates out of and delaminates from the epicardium and then populates the subepicardial matrix as these EPDCs interact with myocardial cells and undergo EMT (18, 49). We immunohistochemically examined human TBX5 expression in the epicardium and subepicardium during human fetal cardiac development. Compared with the marked TBX5 staining in the static epicardium or intramyocardial vasculature, the subepicardial layer of migrating EPDCs was devoid of TBX5 staining (Fig. 2); previous studies by others have suggested that this area is composed of delaminating EPDCs (18, 49).

Given the common developmental origins of the coronary vasculature and epicardium and the critical role of these cell populations in the establishment of the cardiac conduction system (18, 49), we sought to determine in the chick whether *cTbx5* is expressed in the PEO. In situ hybridization with a chick *Tbx5*-specific riboprobe revealed specific *Tbx5* expression in the developing chick PEO (Fig. 3) similar to previous findings of *Tbx5* in the murine septum transversum (62). Notably, expression of *Tbx5* in the PEO and primitive ventricles is lower compared with that observed in the primitive atria and wing buds. Heterogeneity of *Tbx5* expression in the PEO was also observed, with the aspect in contact with the primitive atrium exhibiting the highest level of expression. In addition, PEOs, myocardium, and tail bud were microdissected from 14 HH stage 16–18 chick embryos, and RNA samples were prepared. RT-PCR demonstrated that *cTbx5* is expressed not

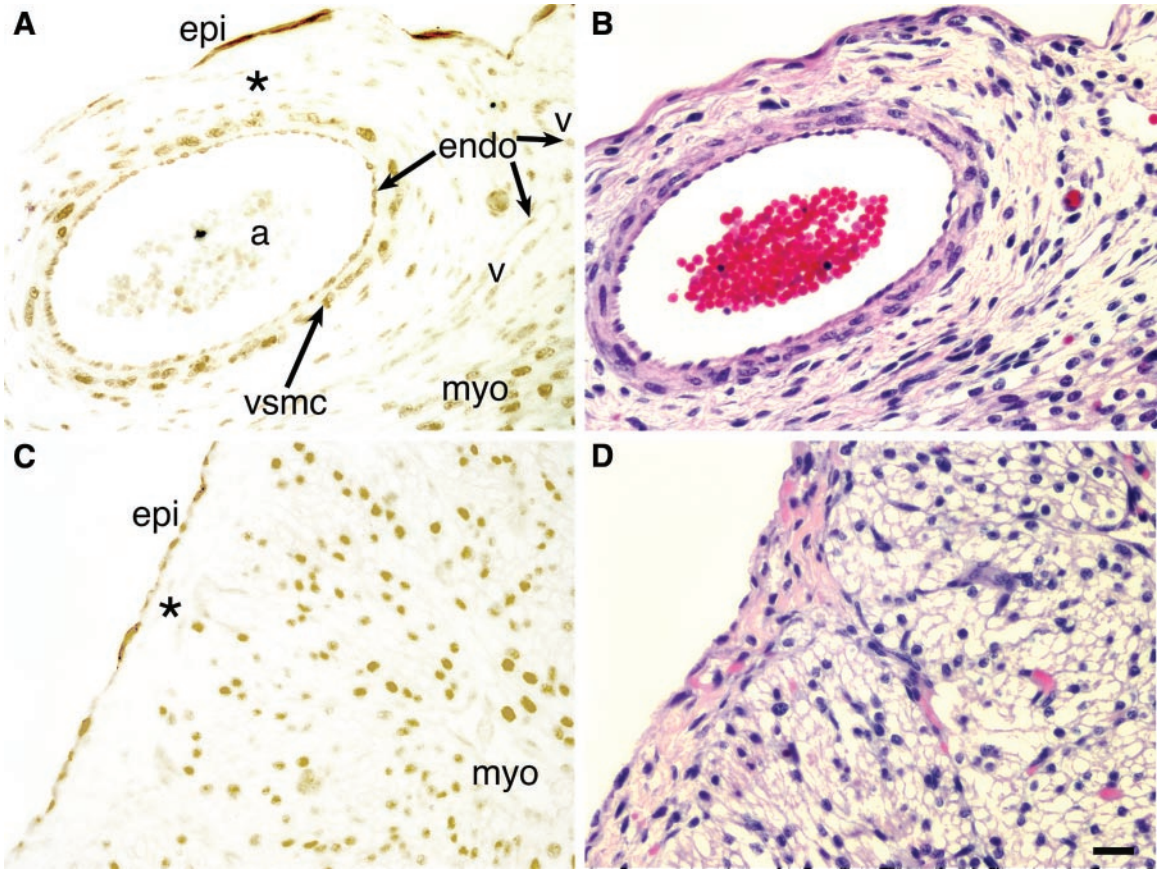

Fig. 2. TBX5 is not expressed in the subepicardium of the embryonic human heart. Immunostaining for TBX5 was performed in 15 wk of gestation human heart. Shown are sections through the lateral wall of the embryonic left ventricle (*A* and *B*) and through the right atrial free wall (*C* and *D*). Immunohistochemistry with anti-TBX5 is shown in *A* and *C*. Although TBX5 is expressed in epicardial, vascular, and myocardial cells, the subepicardium (*), comprised of delaminating epicardial-derived cells (EPDCs) that will ultimately form the nonmigrating vasculature, is devoid of TBX5 expression. Labels indicate epicardium (epi), myocardium (myo), arteriole (a), vein (v), vascular endothelial cells (endo), and vascular smooth muscle cells (vsmc). Hematoxylin and eosin staining of parallel sections (*B* and *D*) demonstrates the cellularity of the subepicardium. Bar = 25 μm.

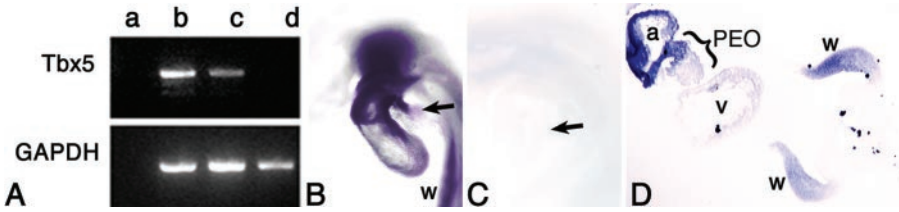

Fig. 3. Analysis of cTbx5 expression in the embryonic chick heart and proepicardial organ (PEO). *A*: total RNA was prepared from Hamburger-Hamilton (HH) stage 16–18 embryonic chick myocardium (*lane b*), PEO (*lane c*), and tail bud (*lane d*). The 887-bp and 806-bp segments of the chick *Tbx5* and *GAPDH* genes, respectively, were amplified by RT-PCR. *cTbx5* is expressed in both the myocardium and PEO, but not in the tail bud. *Lane a* is a negative RT-PCR control in which RNA was omitted from the sample undergoing amplification. *B*: in situ hybridization analysis of HH stage 17 chick embryo with an antisense *cTbx5*-specific riboprobe. *cTbx5* mRNA expression was observed in the PEO (arrow) as well as in the wing bud (w) and heart. *C*: embryos hybridized with a sense *cTbx5* riboprobe showed no staining of the PEO (arrow). *D*: cross-sectional analysis of an HH stage 17 chick embryo confirmed *cTbx5* expression in the PEO, as well as in the wing buds (w) and primitive atrium (a) and ventricle (v).

only in the myocardium but also in the PEO (Fig. 3). No *cTbx5* expression was observed in the tail bud.

Overexpression of TBX5 in the PEO. To determine whether regulation of Tbx5 dose plays a role in PEO development and its progenitors, we used retrovirus-mediated transgenesis to augment Tbx5 expression in the PEO during chick development. CXIZ retroviruses encoding either β-galactosidase alone or in addition to human TBX5 isoforms (wild-type or Gly80Arg mutant) were microinjected into the PEO of HH stage 16–18 embryonic chicks in ovo. Embryos were killed and studied at embryonic *day 15* (*E15*) by whole mount staining for β-galactosidase (Fig. 4) and light microscopy (Fig. 5). CXIZ-injected embryos exhibited β-galactosidase-positive cells in both the epicardium (Figs. 4, *A–C*) as well as the vascular smooth muscle and surrounding endothelium of the coronary vasculature (Figs. 5, *A* and *B*). Mosaic staining confirmed previous findings (23, 49, 71) that this retroviral strategy results in transgenesis of a portion of the targeted cells. Although epicardium and coronary vasculature did form in wt-TBX5-CXIZ-injected embryos (Fig. 4*F*), we did not observe significant incorporation of β-galactosidase-positive cells into these structures (Figs. 5, *C* and *D*). Microinjection of the inactive mutant Gly80Arg-TBX5-CXIZ (23) revealed a pattern of β-galactosidase-positive cell expression similar to that found in CXIZ-injected embryos (Fig. 4, *D* and *E*). Therefore, we concluded that overexpression of biologically active TBX5 specifically inhibits incorporation of proepicardial cells into epicardium and coronary vasculature.

Does TBX5 modulate proepicardial cell proliferation and migration in vitro? Because our previous studies (23) had demonstrated that TBX5 can act as a growth-arrest signal to inhibit the proliferation of several cell types including D17 cells, MEQC *myc*-transformed avian cardiomyocyte-like cells (26), and embryonic chick cardiomyocytes, we considered the possibility that TBX5 overexpression might inhibit the proliferation of a subset of proepicardial cells within the PEO and thereby prevent their clonal expansion and further incorporation into PEO-derived structures. However, immunostaining for PCNA in PEOs infected with either CXIZ or wt-TBX5-CXIZ both revealed evidence of proliferation in virtually all cells. To further quantitatively determine whether TBX5 overexpression altered proepicardial cell proliferation, primary cultures of proepicardial cells were established by disaggregating PEOs microdissected from HH stage 16–18 chick embryos.

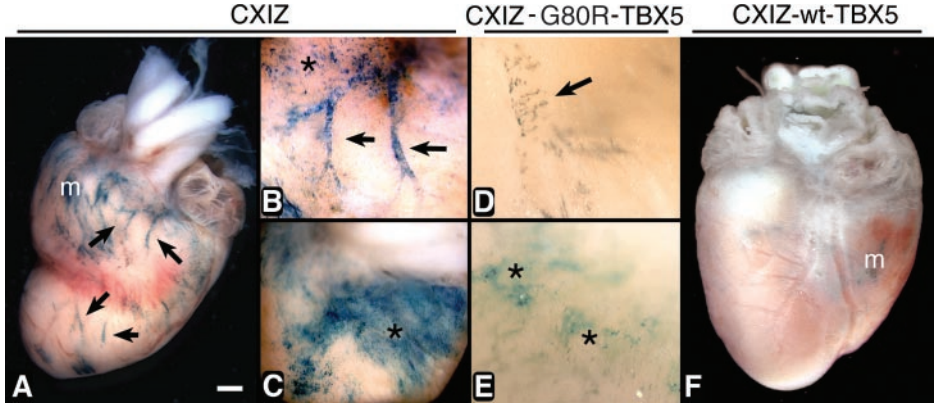

Fig. 4. Retrovirus-mediated expression of wild-type and mutant human TBX5 in embryonic chick PEO during heart development. CXIZ (*A–C*), Gly80Arg-TBX5-CXIZ (*D* and *E*), and wt-TBX5-CXIZ (*F*) retroviruses were microinjected into chick PEOs in ovo at HH stage 16–18. Embryos were euthanized at embryonic *day 15* (*E15*), and whole mounts were stained (blue) for β-galactosidase. Microscopic inspection revealed widespread expression of the transgene in the epicardial cell layer (∗) and underlying coronary vessels (arrows) in the CXIZ-infected (*A–C*) and Gly80Arg-TBX5-CXIZ-infected (*D* and *E*) hearts. *F*: in wt-TBX5-CXIZ-infected hearts, staining of the epicardium and coronary vasculature was not detected. In all cases, minimal myocyte expression of the transgene (m) is observed due to leakage of the retrovirus into the myocardium during pressure microinjection and thus verifies both the infectivity of the retrovirus and expression of the transgene. Bar shown in *A* = 800 μm (for *A* and *F*), or 400 μm (for *B* and *C*), or 100 μm (for *D* and *E*).

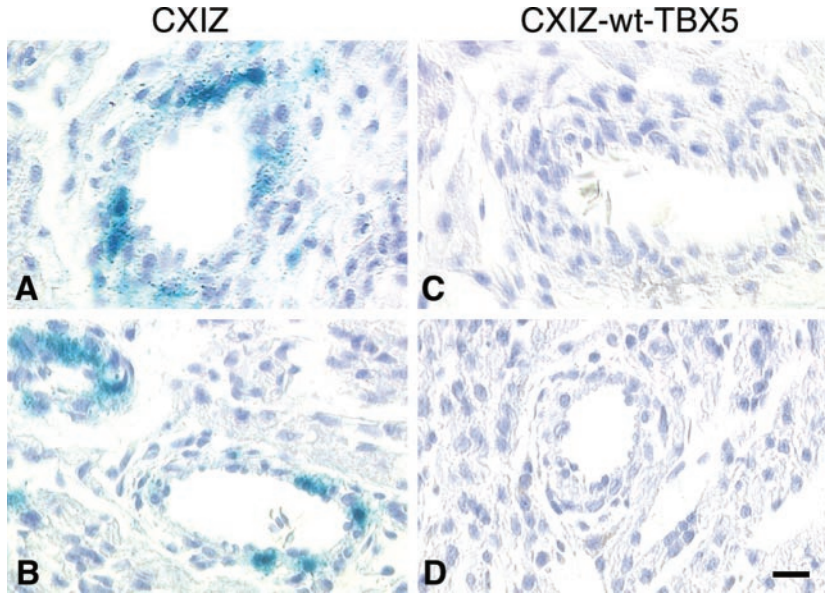

Fig. 5. Histological detection of retrovirus-mediated human TBX5 expression in ovo. Histological sections of embryonic chick hearts stained for β-galactosidase activity after being infected with CXIZ (*A* and *B*) or wt-TBX5-CXIZ (*C* and *D*) retroviruses revealed expression of β-galactosidase in the intimal endothelium and medial smooth muscle of the coronary arteries in CXIZ-microinjected hearts. However, this was undetectable in the wt-TBX5-CXIZ hearts. Bar = 20 μm.

Cultures were infected with CXIZ, wt-TBX5-CXIZ, or Gly80Arg-TBX5-CXIZ retroviruses and then fixed and immunostained for PCNA within 24 h of initial proepicardial cell plating. These studies demonstrated no significant difference in the fraction of PCNA-positive cells regardless of TBX5 isoform overexpression (data not shown). Quantitation of these studies is shown in Fig. 6*A*.

Since our experiments suggested that TBX5 does not significantly alter proepicardial cell proliferation, we tested the hypothesis that TBX5 might inhibit proepicardial cell migration out of the PEO and thereby inhibit incorporation of retrovirus-infected cells into the epicardium and coronary vasculature. Because it had been previously suggested that TBX5 regulation of cell migration might play a role in establishment of the limb bud (2), we first sought to determine whether TBX5 inhibited in vitro migration of D17 cells. Osteosarcoma cell activity in vitro has been previously utilized as an experimental model of bone formation (44, 61). We had previously shown that TBX5 inhibited D17 cell proliferation, but recent data has suggested that the effects of TBX5 on cell migration and cell proliferation might contribute to limb development (2). D17 cells were infected with CXIZ, wt-TBX5-CXIZ, or Gly80Arg-TBX5-CXIZ retroviruses. Infected cells were allowed to migrate in culture for 10 days in the presence of hydroxyurea, a potent inhibitor of cell proliferation. Quantification of cell migration (Fig. 6*B*) revealed that wt-TBX5-CXIZ-infected D17 cells migrated significantly less than D17 cells infected with CXIZ or Gly80Arg-TBX5-CXIZ ($P < 0.0001$). To determine whether TBX5-mediated inhibition of cell migration was cell-autonomous, we assessed the migration of CXIZ-infected D17 cells cocultured with D17 cells infected with wt-TBX5-CXIZ. Cultures analyzed contained 0, 14, or 41% wt-TBX5-CXIZ-infected D17 cells, so the majority of cells at the migrating front would be CXIZ-infected D17 cells. After 10 days of coculture, we did not observe (Fig. 6*C*) significant alterations ($P = 0.9$) in D17 migration regardless of the amount of wt-TBX5-CXIZ-infected D17 cells present. Therefore, we concluded that TBX5 inhibited D17 cell migration in vitro in a cell-autonomous fashion.

Because D17 osteosarcoma cell behavior may not mimic proepicardial cell behavior, we explored the consequences of TBX5 overexpression on proepicardial cell migration. Explanted PEOs were either infected in culture with CXIZ, wt-TBX5-CXIZ, or Gly80Arg-TBX5-CXIZ retroviruses for 24 h and maintained for a further 48 h in virus-free media, or they were transfected with pEGFP-C1 or pEGFP-C1-TBX5 for 4 h and then maintained in normal media for a further 24 h. Migration of cells was assessed by β-galactosidase staining in retrovirus-infected cultures or by fluorescence microscopy in plasmid-transfected cultures. As previously described (30), proepicardial cells migrated out of the PEO in a radial fashion during culture of explanted PEOs. In CXIZ- and Gly80Arg-TBX5-CXIZ-infected cultures, 88 and 91%, respectively, of β-galactosidase-positive cells had migrated out of the explant (Fig. 7*A*). By contrast, only 25% of β-galactosidase-positive cells were seen in the wt-TBX5-CXIZ migrating population, and most remained within the explanted PEO (Fig. 7*A*). Notably, even though a minority of proepicardial cells were infected by the retrovirus, there was no evidence of inhibition of migration of noninfected cells out of the PEO. In cultures transfected with pEGFP-C1 plasmid alone, 81% of EGFP-positive cells migrated out of the explant (Fig. 7*B*). However, in pEGFP-C1-TBX5-transfected cultures, only 32% of EGFP-positive cells migrated out of the explant, while the majority remained within the explanted PEO (Fig. 7*C*). Not only do these data support the hypothesis that TBX5 overexpression inhibits proepicardial cell migration, but these data also confirm that this effect is cell autonomous.

We further considered whether TBX5 activity is essential for proepicardial cell migration. To evaluate this hypothesis, we determined the consequences of loss of cTbx5 activity on proepicardial cell migration in vitro by treatment with cTbx5 morpholino antisense oligonucleotides (cTbx5-MO) derived from sequences flanking the cTbx5 consensus Kozak sequence. Similar oligonucleotides have been used by Ng et al. (54), Ahn et al. (2), and Garrity et al. (16) to inhibit Tbx5 translation during zebrafish pectoral limb bud and heart development. PEO explants were transfected with cTbx5-MO or a control

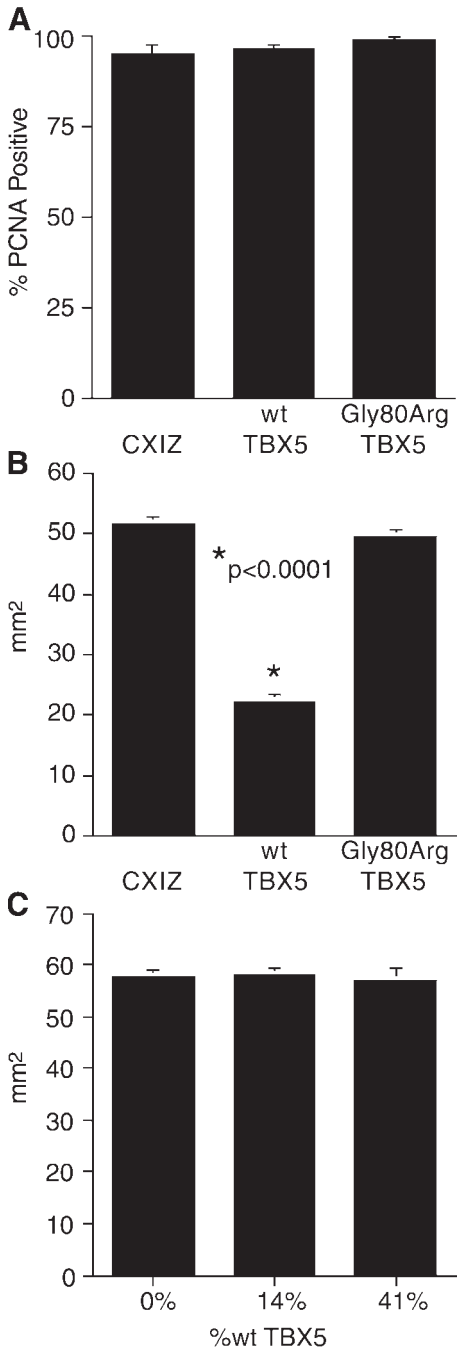

Fig. 6. Effect of TBX5 overexpression on proepicardial cell proliferation and D17 cell migration in vitro. *A*: primary cultures of proepicardial cells were infected with CXIZ, wt-TBX5-CXIZ, or Gly80Arg-TBX5-CXIZ retroviruses and immunostained with anti-PCNA 24 h after initial plating to determine the fraction of proliferating cells. No significant effect of TBX5 on PEO cell proliferation was observed ($P = 0.532$). *B*: migration rates of D17 cells infected with CXIZ, wt-TBX5-CXIZ, or Gly80Arg-TBX5-CXIZ retroviruses were determined during a 10-day sheet migration assay. Compared with CXIZ and Gly80Arg-TBX5-CXIZ retroviruses, infection of D17 cells with wt-TBX5-CXIZ significantly inhibits migration ($P < 0.0001$). *C*: D17 cells infected with CXIZ were cocultured with D17 cells infected with wt-TBX5-CXIZ at varied fractions and subjected to a 10-day sheet migration assay. Increasing proportions of wt-TBX5-CXIZ-infected D17 cells produced no significant differences ($P = 0.9$) in D17 migration.

antisense oligomer comprising the same sequence, but in an inverted orientation (cTbx5-INV). Since both oligomers were covalently tagged with Lissamine, transfection efficiency was assessed by fluorescent microscopy, and 40–50% of cells incorporated both oligomers. Proepicardial cell migration was assessed after 24 h in culture. In explants treated with either cTbx5-MO or cTbx5-INV, we observed no change in migration of proepicardial cells that did not take up the antisense oligomers. However, migration of cTbx5-MO-transfected proepicardial cells was markedly inhibited compared with the migration of cTbx5-INV-transfected cells; most cTbx5-MO proepicardial cells failed to migrate out of the explanted PEO (Fig. 8). These studies further suggest that not only is the contribution of Tbx5 to cell migration cell autonomous, but also that regulation of Tbx5 expression is required for normal proepicardial cell migration.

TBX5 overexpression inhibits proepicardial cell migration in vivo. To determine whether TBX5 has effects in vivo similar to those effects it has on cell migration in vitro, we analyzed the fate of TBX5-overexpressing proepicardial cells in the developing chick in vivo (Fig. 9). PEOs of HH stages 16–18 embryonic chicks were microinjected with CXIZ, Gly80Arg-TBX5-CXIZ, or wt-TBX5-CXIZ retrovirus, and the embryos were euthanized and stained for β-galactosidase activity at 8, 24, and 48 h following microinjection. In both CXIZ- and wt-TBX5-CXIZ-infected embryos, β-galactosidase staining was evident in the PEO by 8 h postmicroinjection. By 24 h postmicroinjection, CXIZ-infected proepicardial cells were noted to have begun to migrate over the surface of the looping heart and, by 48 h, were observed to incorporate into nascent epicardium and vascular structures. Similar data was obtained for Gly80Arg-TBX5-CXIZ-infected cells (data not shown). However, at these 24 and 48 h time points, wt-TBX5-CXIZ-infected proepicardial cells remained in the PEO and failed to migrate over the heart surface.

Native Tbx5 expression in migrating proepicardial cells. Our studies suggested that disruption of Tbx5 signaling in genetically engineered cells perturbs their capacity for migration. We therefore hypothesized that native Tbx5 expression might be dynamically regulated in cells that alternate between stationary and migratory states during development. To address this, we compared *cTbx5* expression in chick proepicardial cells that were stationary or migrating. PEOs were explanted from 81 HH stage 16–18 chick embryos and maintained in organ culture for 72 h, by which time a subpopulation of proepicardial cells had migrated out of the PEO onto the culture dish while the rest remained within the PEO. From each culture, the residual, nonmigrating PEO was removed by microdissection, and then the migrating proepicardial cells were removed from the dish by trypsinization. RT-PCR analyses of *cTbx5* expression were performed on RNA samples from both populations of cells. These studies revealed that like HH stage 16–18 PEOs in vivo (Fig. 3), the nonmigrating cells from cultured PEOs continued to express *cTbx5* (Fig. 10). However, migrating proepicardial cells no longer expressed detectable levels of *cTbx5* (Fig. 10). Thus migration of proepicardial cells out of the PEOs in this culture model was associated with inactivation of *cTbx5* expression.

Do Tbx18 and Tbx20 contribute to Tbx5 effects on proepicardial cell migration? Concomitant alterations in the expression levels of multiple T-box transcription factors, e.g., Tbx5,

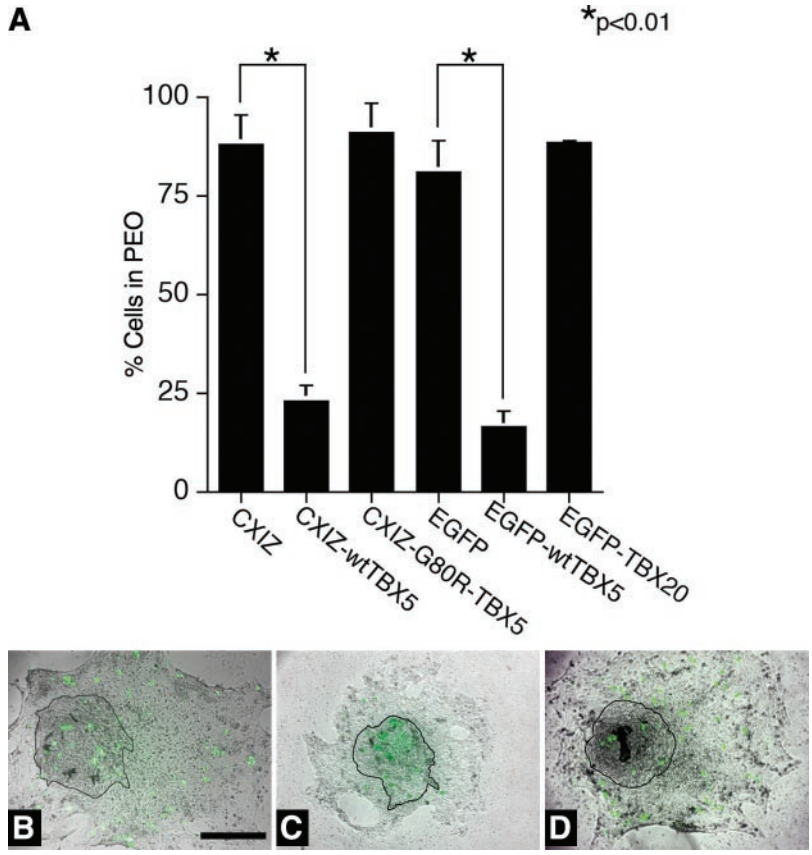

Fig. 7. Effect of TBX5 overexpression on proepicardial cell migration in vitro. The consequences of retroviral- or plasmid-mediated overexpression of TBX5 in explanted PEOs were studied. *A*: quantitative determination of proepicardial cell migration in vitro after infection with CXIZ retrovirus or retrovirus encoding wt-TBX5 or Gly80Arg mutant TBX5. Significant inhibition of migration by wild-type TBX5 but not by Gly80Arg TBX5 was observed. *B*: a PEO explant transfected with pEGFP-C1 is shown under phase microscopy. Most of the transfected cells (green), visualized by fluorescent microscopy, migrate out of the initial PEO explant, outlined in black. *C*: most of the pEGFP-C1-wt-TBX5-transfected cells shown fail to migrate out of the PEO explant. *D*: most of the pEGFP-C1-TBX20-transfected cells shown migrate out of the PEO explant. Bar = 300 μm for *B–D*.

Tbx2, Tbx3, and Tbx20, have been suggested to play a role in myocardial development (10a, 57), and our observations of proepicardial cell behavior may not be solely due to Tbx5 but rather imbalances of several PEO T-box genes. Both Tbx18 and Tbx20 have been implicated in vascular development and are expressed in the PEO/septum transversum (8, 28). We used quantitative RT-PCR to determine whether proepicardial expression of *Tbx18* and *Tbx20* changed in response to *Tbx5* knockdown via antisense inhibition of *Tbx5* expression as described above. *Tbx18* expression was not significantly changed in PEO cultures treated with cTbx5-MO compared with those treated with cTbx5-INV (1.3 ± 0.2 x). However, Tbx5 knockdown was associated with a significant increase (1.9 ± 0.3 ×) in *Tbx20* expression. Recently, Plageman et al. (57) suggested that maintenance of Tbx5 and Tbx20 balance may be critical for myocardial development. To determine whether proepicardial cell migration was similarly regulated, we directly tested the effect of altered *Tbx20* expression on proepicardial cell migration. We studied the consequences of both Tbx20 knockdown (using morpholino antisense oligonucleotides) and Tbx20 overexpression (using pEGFP-C1-TBX20 plasmids; see Fig. 7, *A* and *D*) on proepicardial cell migration out of cultured PEO explants just as we had for Tbx5. We found that 83% and 89% of proepicardial cells subject to cTbx20 knockdown or TBX20 overexpression, respectively, migrated out of the proepicardial explant. These proportions were similar to the high proportion of migrating cells seen in control cultures treated with inverted cTbx20 antisense oligomers (82%) or pEGFP-C1 plasmid (81%) but significantly differed ($P < 0.01$) from the low proportion of cells that migrated out of the proepicardial explant in cultures treated with cTbx5 antisense oligomers (42%) or with pEGFP-C1-wt-TBX5 (16%).

DISCUSSION

In this study, we demonstrate that TBX5 is expressed in the PEO, which contains epicardial and coronary vascular progenitor cells, and that TBX5 inhibits proepicardial cell migration in vitro and in vivo. Mosaic overexpression of TBX5 in the PEO in vivo during cardiogenesis inhibits proepicardial cell migration out of the PEO with consequent impaired incorporation of transgenic cells into the epicardium and coronary blood vessels. Proepicardial cell migration in vitro is affected by changes in *TBX5* dosage and genetically engineered augmentation or inhibition of TBX5 expression both inhibit proepicardial cell migration. Furthermore, analyses of cultured chick proepicardial cells and of human fetal tissues suggest that physiological regulation of TBX5 expression may occur in vivo in concert with both initiation and cessation of cell migration during embryogenesis. Since we do not observe TBX5 expression in migrating proepicardial cells, our studies suggest that there may be distinct temporal requirements for TBX5 and that our genetic manipulations impair proepicardial cell migration by modifying TBX5 expression in the premigratory cells of the PEO.

We have previously shown that TBX5 inhibits cardiomyocyte proliferation during myocardial development (23). Our data now extend the profile of TBX5 activity to include regulation of migration and indicate that inhibition of migra-

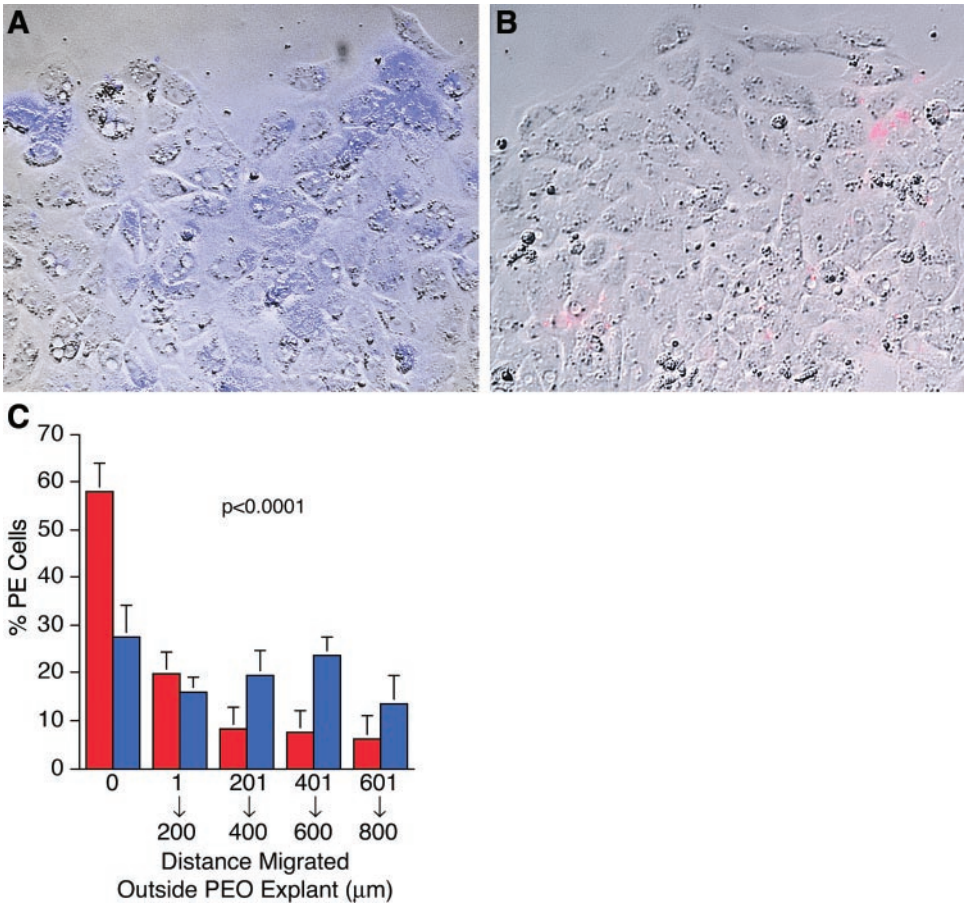

Fig. 8. Antisense suppression of cTbx5 inhibits proepicardial cell migration in vitro. Fluorescence microscopy of proepicardial explants 24 h after being transfected with cTbx5-MO antisense oligonucleotide (*A*) or the cTbx5-INV control oligonucleotide (*B*) reveals that cTbx5 suppression prevents treated cells from migrating out of the explanted organ. Leading edges of migration are shown, and direction of migration is toward the *top*. Transfected cells (blue in *A*, red in *B*) are detected by fluorescence microscopy. *C*: quantitative analysis demonstrates that unlike cTbx5-INV-transfected cells (blue) that migrate progressively out of the proepicardial explant, cTbx5-MO-transfected cells (red) largely remain in the PEO explant, and concentric rings further from the explant contain fewer and fewer cTbx5-MO-transfected cells. Shown are the percentages of transfected proepicardial cells in each culture that are located within the explant (i.e., 0 μm migrated) or at varying distances outside the explant (1–200 μm, 201–400 μm, 301–600 μm, or 601–800 μm).

tion by TBX5 is partially independent of this transcription factor's effects on cell proliferation. Analyses of PCNA expression in TBX5 transgenic chick proepicardial cells demonstrate no effect of TBX5 on proepicardial cell proliferation. Furthermore, unlike TBX5 inhibition of proliferation, TBX5 inhibition of migration is cell autonomous. Coculture of D17 cells with D17 cells genetically engineered to overexpress TBX5 fails to modify their migration in vitro. Although TBX5

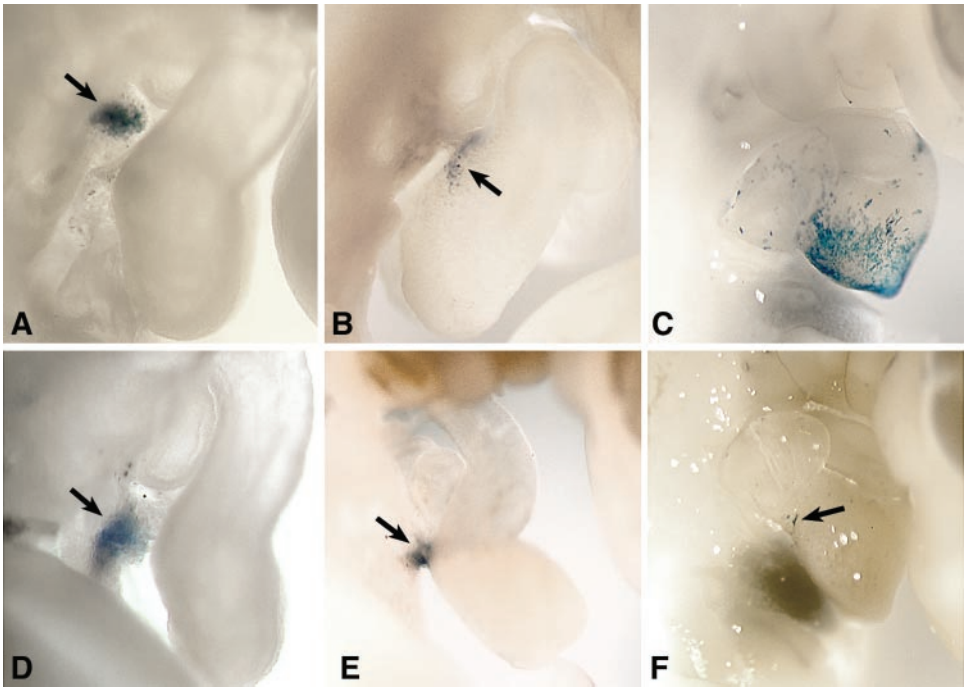

Fig. 9. Effect of TBX5 overexpression on proepicardial cell migration in vivo. At 8 h (*A* and *D*), 24 h (*B* and *E*), and 48 h (*C* and *F*) following microinjection of PEOs in ovo with CXIZ (*A–C*) or wt-TBX5-CXIZ (*D–F*) retroviruses, chick embryos were euthanized, fixed, and stained for β-galactosidase activity. *A* and *D*: β-galactosidase staining (arrows) was evident in PEOs 8 h postmicroinjection, regardless of which retrovirus was injected. *B*: by 24 h postmicroinjection, CXIZ-infected proepicardial cells (arrow) began migrating out of the PEO and onto the surface of the naked myocardium. *C*: by 48 h, the PEO had involuted, and CXIZ-infected proepicardial cells had incorporated into the epicardium and underlying coronary vessels. *E*: however, at 24 h postmicroinjection of wt-TBX5-CXIZ into embryos, infected proepicardial cells (arrow) remained in the PEO. *F*: by 48 h, only rare wt-TBX5-CXIZ-infected proepicardial cells (arrow) were evident outside of the now involuted PEO.

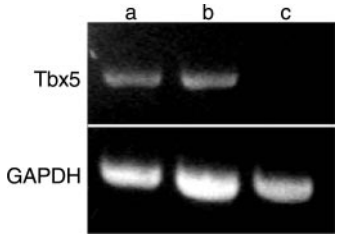

Fig. 10. RT-PCR analysis of cTbx5 expression in embryonic chick PEO explants and migrating proepicardial cells. After 72 h in culture, proepicardial cells migrated onto the culture dish out of PEO explants. These explants were microdissected from the culture dish, and separate RNA pools were prepared from the residual stationary PEO and the migrating proepicardial cells. RT-PCR analyses for *cTbx5* and *cGAPDH* were performed as in Fig. 2 from RNA derived from chick myocardium (*lane a*; positive control for *cTbx5* and *cGAPDH* expression), PEO explant (*lane b*), and migrating proepicardial cells (*lane c*). *cTbx5* is expressed in the residual nonmigrating PEO explant (*lane b*) but not in the migratory proepicardial cells (*lane c*).

overexpression retards proepicardial cell migration out of cultured PEO explants, migration of nontransgenic cells out of the same PEOs is not impeded. Moreover, in the setting of mosaic overexpression of TBX5 in the chick PEO, further cardiogenic development does support the establishment of epicardium and coronary vasculature from nontransgenic cells.

TBX5 modulation of cell differentiation has been reported in both the heart and the limb. In this study, inhibition of proepicardial cell migration occurs before the differentiating events that constitute EMT and prevents the physical interaction of EPDCs with myocardial cells that is required for EMT. Thus we hypothesize that TBX5 regulation of cell migration is also independent of its effects on cell differentiation. However, we cannot exclude TBX5 modulation of early, as yet uncharacterized, differentiating events that might occur within the PEO before cells migrate over and into the myocardium.

Investigation of the role of Tbx5 in zebrafish fin development also suggests independent contributions of Tbx5 to regulation of cell migration, proliferation, and differentiation. Although there is a clear role for Tbx5 in cell differentiation and proliferation during limb specification, Ahn et al. (2) demonstrated that the contribution of Tbx5 to limb development commences prior to limb bud formation. Antisense knockdown of Tbx5 impairs mesenchymal aggregation of limb precursor cells and, in a cell-autonomous fashion, prevents lateral plate mesodermal cells from migrating to the nascent pectoral fin bud. Cell adhesive properties may also be changed during fin development in response to altered *Tbx5* dose, and likewise, defective proepicardial cell adhesion during migration out of the PEO may contribute to the impaired epicardial formation and coronary vasculogenesis in our chick studies. Altered dosage of other T-box transcription factors has also been shown to modify cell migration. Loss of Tbx16 in the zebrafish *spadetail* mutant causes a cell-autonomous distorted convergence of marginal mesodermal cells during gastrulation (20). Wilson et al. (72) proposed that abnormal notochord morphogenesis in the setting of loss of *T(Brachyury)* is a consequence of a defective migration of posterior mesodermal cells through the primitive streak that may involve abnormal cell adhesive properties. Future studies to decipher mechanisms underlying TBX5 inhibition of proepicardial cell migration will explore potential regulation of cell-cell adhesion molecules such as VCAM-1 (31) and BVES (70) and cell-matrix adhesion molecules such as α4-integrin (73) that are associated with proepicardial development (59), as well as transcriptional regulators of epicardial EMT such as Ets-1 and Ets-2 (35).

The molecular genetic events downstream from Tbx5 that contribute to regulation of cell migration and EMT remain to be defined. FGF isoforms (1, 2, and 7), TGFβ isoforms (1, 2, and 3), Ets-1, Ets-2, and Fog2 have all been implicated in coronary vasculogenesis and cardiac EMT (35, 50, 64, 69). Related molecules have all been tied to T-box gene activity in other experimental models. FGF10 has been proposed to be a downstream target of Tbx5 in murine limb development (1, 54). In *Drosophila*, the TGFβ homolog *decapentaplegic* acts to regulate expression of the T-box gene *optomotor blind* during development of the wing imaginal disc (52). GATA-4 (the binding partner of Fog2) interacts with Tbx5 and Nkx2.5 to activate synergistically expression of the atrial natriuretic factor gene (15, 55, 68), and Gata-4 expression is altered in *Tbx5* homozygous null mice (10). Thus these are all intriguing candidate members of a Tbx5-dependent pathway operant in proepicardial cells and their descendants.

Although our data exclude altered *Tbx18* and *Tbx20* expression as explanations for Tbx5-mediated modulation of proepicardial cell migration, these data do not exclude a role in other proepicardial cell behaviors including proliferation and differentiation. Nor do our data exclude a role for Tbx5 in these other properties either. Additionally, the observation that antisense knockdown of Tbx5 inhibits proepicardial cell migration while proepicardial physiological inactivation of Tbx5 expression is associated with promotion of cell migration suggests that non-Tbx5-dependent pathways are operant in vivo as well. Human and animal genetic studies have previously predicted that T-box gene dose is finely regulated in normal development, and perturbations that either increase or decrease T-box gene dose lead to abnormal organogenesis. Murine models of overexpression or haploinsufficiency of *Tbx1* all lead to aortic arch abnormalities that are also seen in humans with DiGeorge syndrome who have deletions encompassing the *Tbx1* gene (19, 27, 36, 46). Abnormal cardiogenesis is a feature of murine models of *Tbx5* overexpression and haploinsufficiency (10, 34) and is similar to the human congenital heart disease seen in Holt-Oram patients with *TBX5* haploinsufficiency and in humans with chromosome 12q2 duplications that include *TBX5* (3, 32). Vascular anomalies (patent ductus arteriosus, persistent left superior vena cava, anomalous pulmonary venous return, aortic coarctation) have been variably noted in these human patients and animal models, but coronary artery anatomy has not been well studied in these individuals. TBX5 and other members of TBX5-dependent pathways in PEO development will be appropriate candidates for genetic analyses in individuals with coronary artery and epicardial anomalies.

ACKNOWLEDGMENTS

We are grateful to Andy Wessels, Maurice J. B. van den Hoff, David Reese, Romulo Hurtado, and Theresa Zagreda for advice regarding PEO manipulation and histological analysis.

GRANTS

This work was supported by the March of Dimes Birth Defects Foundation (to C. T. Basson), the Edward Mallinckrodt, Jr. Foundation (to C. T. Basson), the Cornell Vascular Medicine Foundation (to C. T. Basson), National Heart,

Lung, and Blood Institute (NHLBI) Grant R01-HL-66214 (to C. T. Basson), and by an NHLBI Minority Investigator Research Award (to C. J. Hatcher).

REFERENCES

1. **Agarwal P, Wylie JN, Galceran J, Arkhitko O, Li C, Deng C, Grosschedl R, and Bruneau BG.** Tbx5 is essential for forelimb bud initiation following patterning of the limb field in the mouse embryo. *Development* 130: 623–633, 2003.
2. **Ahn DG, Kourakis MJ, Rohde LA, Silver LM, and Ho RK.** T-box gene tbx5 is essential for formation of the pectoral limb bud. *Nature* 417: 754–758, 2002.
3. **Basson CT, Bachinsky DR, Lin RC, Levi T, Elkins JA, Soults J, Grayzel D, Kroumpouzou E, Traill TA, Leblanc-Straceski J, Renault B, Kucherlapati R, Seidman JG, and Seidman CE.** Mutations in human TBX5 cause limb and cardiac malformation in Holt-Oram syndrome. *Nat Genet* 15: 30–35, 1997.
4. **Basson CT, Knowles WJ, Bell L, Albelda SM, Castronovo V, Liotta LA, and Madri JA.** Spatiotemporal segregation of endothelial cell integrin and nonintegrin extracellular matrix-binding proteins during adhesion events. *J Cell Biol* 110: 789–801, 1990.
5. **Basson CT, Kocher O, Basson MD, Asis A, and Madri JA.** Differential modulation of vascular cell integrin and extracellular matrix expression in vitro by TGF-beta 1 correlates with reciprocal effects on cell migration. *J Cell Physiol* 153: 118–128, 1992.
6. **Begemann G and Ingham PW.** Developmental regulation of Tbx5 in zebrafish embryogenesis. *Mech Dev* 90: 299–304, 2000.
7. **Bray N, Dubchak I, and Pachter L.** AVID: A global alignment program. *Genome Res* 13: 97–102, 2003.
8. **Brown DD, Binder O, Pagratis M, Parr BA, and Conlon FL.** Developmental expression of the *Xenopus laevis* Tbx20 orthologue. *Dev Genes Evol* 212: 604–607, 2003.
9. **Bruneau BG, Logan M, Davis N, Levi T, Tabin CJ, Seidman JG, and Seidman CE.** Chamber-specific cardiac expression of Tbx5 and heart defects in Holt-Oram syndrome. *Dev Biol* 211: 100–108, 1999.
10. **Bruneau BG, Nemer G, Schmitt JP, Charron F, Robitaille L, Caron S, Conner DA, Gessler M, Nemer M, Seidman CE, and Seidman JG.** A murine model of Holt-Oram syndrome defines roles of the T-box transcription factor Tbx5 in cardiogenesis and disease. *Cell* 106: 709–721, 2001.

10a. **Christoffels VM, Hoogaars WM, Tessari A, Clout DE, Moorman AF, and Campione M.** T-box transcription factor Tbx2 represses differentiation and formation of the cardiac chambers. *Dev Dyn* 229: 763–770, 2004.

11. **Collavoli A, Hatcher CJ, He J, Okin D, Deo R, and Basson CT.** TBX5 nuclear localization is mediated by dual cooperative intramolecular signals. *J Mol Cell Cardiol* 35: 1191–1195, 2003.
12. **Crispino JD, Lodish MB, Thurberg BL, Litovsky SH, Collins T, Molkentin JD, and Orkin SH.** Proper coronary vascular development and heart morphogenesis depend on interaction of GATA-4 with FOG cofactors. *Genes Dev* 15: 839–844, 2001.
13. **Drabkin HA, Parsy C, Ferguson K, Guilhot F, Lacotte L, Roy L, Zeng C, Baron A, Hunger SP, Varella-Garcia M, Gemmill R, Brizard F, Brizard A, and Roche J.** Quantitative HOX expression in chromosomally defined subsets of acute myelogenous leukemia. *Leukemia* 16: 186–195, 2002.
14. **Dubchak I, Brudno M, Loots GG, Pachter L, Mayor C, Rubin EM, and Frazer KA.** Active conservation of noncoding sequences revealed by three-way species comparisons. *Genome Res* 10: 1304–1306, 2000.
15. **Garg V, Kathiriya IS, Barnes R, Schluterman MK, King IN, Butler CA, Rothrock CR, Eapen RS, Hirayama-Yamada K, Joo K, Matsuoka R, Cohen JC, and Srivastava D.** GATA4 mutations cause human congenital heart defects and reveal an interaction with TBX5. *Nature* 424: 443–447, 2003.
16. **Garrity DM, Childs S, and Fishman MC.** The heartstrings mutation in zebrafish causes heart/fin Tbx5 deficiency syndrome. *Development* 129: 4635–4645, 2002.
17. **Ghosh TK, Packham EA, Bonser AJ, Robinson TE, Cross SJ, and Brook JD.** Characterization of the TBX5 binding site and analysis of mutations that cause Holt-Oram syndrome. *Hum Mol Genet* 10: 1983–1994, 2001.
18. **Gittenberger-de Groot AC, Vrancken Peeters MP, Mentink MM, Gourdie RG, and Poelmann RE.** Epicardium-derived cells contribute a novel population to the myocardial wall and the atrioventricular cushions. *Circ Res* 82: 1043–1052, 1998.
19. **Goldmuntz E and Emanuel BS.** Genetic disorders of cardiac morphogenesis. The DiGeorge and velocardiofacial syndromes. *Circ Res* 80: 437–443, 1997.
20. **Griffin KJ, Amacher SL, Kimmel CB, and Kimelman D.** Molecular identification of spadetail: regulation of zebrafish trunk and tail mesoderm formation by T-box genes. *Development* 125: 3379–3388, 1998.
21. **Hamburger V and Hamilton HL.** A series of normal stages in the development of the chick embryo. *J Morphol* 88: 49–92, 1951.
22. **Hatcher CJ, Goldstein MM, Mah CS, Delia CS, and Basson CT.** Identification and localization of TBX5 transcription factor during human cardiac morphogenesis. *Dev Dyn* 219: 90–95, 2000.
23. **Hatcher CJ, Kim MS, Mah CS, Goldstein MM, Wong B, Mikawa T, and Basson CT.** TBX5 transcription factor regulates cell proliferation during cardiogenesis. *Dev Biol* 230: 177–188, 2001.
24. **Heicklen-Klein A and Evans T.** T-box binding sites are required for activity of a cardiac GATA-4 enhancer. *Dev Biol* 267: 490–504, 2004.
25. **Iio A, Koide M, Hidaka K, and Morisaki T.** Expression pattern of novel chick T-box gene, Tbx20. *Dev Genes Evol* 211: 559–562, 2001.
26. **Jaffredo T, Chestier A, Bachnou N, and Dieterlen-Lievre F.** MC29-immortalized clonal avian heart cell lines can partially differentiate in vitro. *Exp Cell Res* 192: 481–491, 1991.
27. **Jerome LA and Papaioannou VE.** DiGeorge syndrome phenotype in mice mutant for the T-box gene, Tbx1. *Nat Genet* 27: 286–291, 2001.
28. **Kraus F, Haenig B, and Kispert A.** Cloning and expression analysis of the mouse T-box gene Tbx18. *Mech Dev* 100: 83–86, 2001.
29. **Kraus F, Haenig B, and Kispert A.** Cloning and expression analysis of the mouse T-box gene Tbx20. *Mech Dev* 100: 87–91, 2001.
30. **Kubalak SW, Doevendans PA, Rockman HA, Hunter JJ, Tanaka N, Ross J Jr, and Chien KR.** Molecular analysis of cardiac muscle diseases based on mouse genetics. In: *Human Molecular Genetics*, edited by Adolph KW. San Diego, CA: Academic, 1996, p. 470–487.
31. **Kwee L, Baldwin HS, Shen HM, Stewart CL, Buck C, Buck CA, and Labow MA.** Defective development of the embryonic and extraembryonic circulatory systems in vascular cell adhesion molecule (VCAM-1) deficient mice. *Development* 121: 489–503, 1995.
32. **Li QY, Newbury-Ecob RA, Terrett JA, Wilson DI, Curtis AR, Yi CH, Gebuhr T, Bullen PJ, Robson SC, Strachan T, Bonnet D, Lyonnet S, Young ID, Raeburn JA, Buckler AJ, Law DJ, and Brook JD.** Holt-Oram syndrome is caused by mutations in TBX5, a member of the Brachyury (T) gene family. *Nat Genet* 15: 21–29, 1997.
33. **Li WE, Waldo K, Linask KL, Chen T, Wessels A, Parmacek MS, Kirby ML, and Lo CW.** An essential role for connexin43 gap junctions in mouse coronary artery development. *Development* 129: 2031–2042, 2002.
34. **Liberatore CM, Searcy-Schrick RD, and Yutzey KE.** Ventricular expression of tbx5 inhibits normal heart chamber development. *Dev Biol* 223: 169–180, 2000.
35. **Lie-Venema H, Gittenberger-de Groot AC, van Empel LJ, Boot MJ, Kerkdijk H, de Kant E, and DeRuiter MC.** Ets-1 and Ets-2 transcription factors are essential for normal coronary and myocardial development in chicken embryos. *Circ Res* 92: 749–756, 2003.
36. **Lindsay EA, Vitelli F, Su H, Morishima M, Huynh T, Pramparo T, Jurecic V, Ogunrinu G, Sutherland HF, Scambler PJ, Bradley A, and Baldini A.** Tbx1 haploinsufficiency in the DiGeorge syndrome region causes aortic arch defects in mice. *Nature* 410: 97–101, 2001.
37. **Loots GG, Ovcharenko I, Pachter L, Dubchak I, and Rubin EM.** rVista for comparative sequence-based discovery of functional transcription factor binding sites. *Genome Res* 12: 832–839, 2002.
38. **Lu J, Richardson JA, and Olson EN.** Capsulin: a novel bHLH transcription factor expressed in epicardial progenitors and mesenchyme of visceral organs. *Mech Dev* 73: 23–32, 1998.
39. **Lu JR, McKinsey TA, Xu H, Wang DZ, Richardson JA, and Olson EN.** FOG-2, a heart- and brain-enriched cofactor for GATA transcription factors. *Mol Cell Biol* 19: 4495–4502, 1999.
40. **Macias D, Perez-Pomares JM, Garcia-Garrido L, Carmona R, and Munoz-Chapuli R.** Immunoreactivity of the ets-1 transcription factor correlates with areas of epithelial-mesenchymal transition in the developing avian heart. *Anat Embryol (Berl)* 198: 307–315, 1998.
41. **Majka SM and McGuire PG.** Regulation of urokinase expression in the developing avian heart: a role for the Ets-2 transcription factor. *Mech Dev* 68: 127–137, 1997.
42. **Manner J.** Does the subepicardial mesenchyme contribute myocardioblasts to the myocardium of the chick embryo heart? A quail-chick

chimera study tracing the fate of the epicardial primordium. *Anat Rec* 255: 212–226, 1999.
43. **Mayor C, Brudno M, Schwartz JR, Poliakov A, Rubin EM, Frazer KA, Pachter LS, and Dubchak I.** VISTA: visualizing global DNA sequence alignments of arbitrary length. *Bioinformatics* 16: 1046–1047, 2000.
44. **Mealey KL, Barhoumi R, Rogers K, and Kochevar DT.** Doxorubicin induced expression of P-glycoprotein in a canine osteosarcoma cell line. *Cancer Lett* 126: 187–192, 1998.
45. **Meins M, Henderson DJ, Bhattacharya SS, and Sowden JC.** Characterization of the human TBX20 gene, a new member of the T-Box gene family closely related to the Drosophila H15 gene. *Genomics* 67: 317–332, 2000.
46. **Merscher S, Funke B, Epstein JA, Heyer J, Puech A, Lu MM, Xavier RJ, Demay MB, Russell RG, Factor S, Tokooya K, Jore BS, Lopez M, Pandita RK, Lia M, Carrion D, Xu H, Schorle H, Kobler JB, Scambler P, Wynshaw-Boris A, Skoultchi AI, Morrow BE, and Kucherlapati R.** TBX1 is responsible for cardiovascular defects in velo-cardio-facial/DiGeorge syndrome. *Cell* 104: 619–629, 2001.
47. **Mikawa T, Cohen-Gould L, and Fischman DA.** Clonal analysis of cardiac morphogenesis in the chicken embryo using a replication-defective retrovirus. III. Polyclonal origin of adjacent ventricular myocytes. *Dev Dyn* 195: 133–141, 1992.
48. **Mikawa T and Fischman DA.** Retroviral analysis of cardiac morphogenesis: discontinuous formation of coronary vessels. *Proc Natl Acad Sci USA* 89: 9504–9508, 1992.
49. **Mikawa T and Gourdie RG.** Pericardial mesoderm generates a population of coronary smooth muscle cells migrating into the heart along with ingrowth of the epicardial organ. *Dev Biol* 174: 221–232, 1996.
50. **Morabito CJ, Dettman RW, Kattan J, Collier JM, and Bristow J.** Positive and negative regulation of epicardial-mesenchymal transformation during avian heart development. *Dev Biol* 234: 204–215, 2001.
51. **Morcos PA.** Achieving efficient delivery of morpholino oligos in cultured cells. *Genesis* 30: 94–102, 2001.
52. **Nellen D, Burke R, Struhl G, and Basler K.** Direct and long-range action of a DPP morphogen gradient. *Cell* 85: 357–368, 1996.
53. **Nemer G and Nemer M.** Transcriptional activation of BMP-4 and regulation of mammalian organogenesis by GATA-4 and -6. *Dev Biol* 254: 131–148, 2003.
54. **Ng JK, Kawakami Y, Buscher D, Raya A, Itoh T, Koth CM, Rodriguez Esteban C, Rodriguez-Leon J, Garrity DM, Fishman MC, and Izpisua Belmonte JC.** The limb identity gene Tbx5 promotes limb initiation by interacting with Wnt2b and Fgf10. *Development* 129: 5161–5170, 2002.
55. **Ogura T.** Tbx genes and development of vertebrate limb and heart. *1st International Symposium on Etiology and Morphogenesis of Congenital Cardiovascular Disease in the Post-Genomic Era*, edited by Nakazawa M. Tokyo, Japan: Sankei, 2002, p. 48–49.
56. **Paxton C, Zhao H, Chin Y, Langner K, and Reecy J.** Murine Tbx2 contains domains that activate and repress gene transcription. *Gene* 283: 117–124, 2002.
57. **Plageman TF Jr and Yutzey KE.** Differential expression and function of Tbx5 and Tbx20 in cardiac development. *J Biol Chem* 279: 19026–19034, 2004.
58. **Pratt BA, Harris AS, Morrow JS, and Madri JA.** Mechanisms of cytoskeletal regulation: modulation of aortic endothelial cell spectrin by the extracellular matrix. *Am J Pathol* 117: 349–354, 1984.
59. **Reese DE, Mikawa T, and Bader DM.** Development of the coronary vessel system. *Circ Res* 91: 761–768, 2002.
60. **Rosenthal N and Xavier-Neto J.** From the bottom of the heart: anteroposterior decisions in cardiac muscle differentiation. *Curr Opin Cell Biol* 12: 742–746, 2000.
61. **Shoieb AM, Hahn KA, and Barnhill MA.** An in vivo/in vitro experimental model system for the study of human osteosarcoma: canine osteosarcoma cells (COS31) which retain osteoblastic and metastatic properties in nude mice. *In Vivo* 12: 463–472, 1998.
62. **Stennard FA, Costa MW, Elliott DA, Rankin S, Haast SJ, Lai D, McDonald LP, Niederreither K, Dolle P, Bruneau BG, Zorn AM, and Harvey RP.** Cardiac T-box factor Tbx20 directly interacts with Nkx2–5, GATA4, and GATA5 in regulation of gene expression in the developing heart. *Dev Biol* 262: 206–224, 2003.
63. **Svensson EC, Huggins GS, Dardik FB, Polk CE, and Leiden JM.** A functionally conserved N-terminal domain of the friend of GATA-2 (FOG-2) protein represses GATA4-dependent transcription. *J Biol Chem* 275: 20762–20769, 2000.
64. **Svensson EC, Huggins GS, Lin H, Clendenin C, Jiang F, Tufts R, Dardik FB, and Leiden JM.** A syndrome of tricuspid atresia in mice with a targeted mutation of the gene encoding Fog-2. *Nat Genet* 25: 353–356, 2000.
65. **Svensson EC, Tufts RL, Polk CE, and Leiden JM.** Molecular cloning of FOG-2: a modulator of transcription factor GATA-4 in cardiomyocytes. *Proc Natl Acad Sci USA* 96: 956–961, 1999.
66. **Szeto DP, Griffin KJ, and Kimelman D.** HrT is required for cardiovascular development in zebrafish. *Development* 129: 5093–5101, 2002.
67. **Takebayashi-Suzuki K, Yanagisawa M, Gourdie RG, Kanzawa N, and Mikawa T.** In vivo induction of cardiac Purkinje fiber differentiation by coexpression of preproendothelin-1 and endothelin converting enzyme-1. *Development* 127: 3523–3532, 2000.
68. **Takeuchi JK, Ohgi M, Koshiba-Takeuchi K, Shiratori H, Sakaki I, Ogura K, Saijoh Y, and Ogura T.** Tbx5 specifies the left/right ventricles and ventricular septum position during cardiogenesis. *Development* 130: 5953–5964, 2003.
69. **Tevosian SG, Deconinck AE, Tanaka M, Schinke M, Litovsky SH, Izumo S, Fujiwara Y, and Orkin SH.** FOG-2, a cofactor for GATA transcription factors, is essential for heart morphogenesis and development of coronary vessels from epicardium. *Cell* 101: 729–739, 2000.
70. **Wada AM, Reese DE, and Bader DM.** Bves: prototype of a new class of cell adhesion molecules expressed during coronary artery development. *Development* 128: 2085–2093, 2001.
71. **Wei Y and Mikawa T.** Fate diversity of primitive streak cells during heart field formation in ovo. *Dev Dyn* 219: 505–513, 2000.
72. **Wilson V, Manson L, Skarnes WC, and Beddington RS.** The T gene is necessary for normal mesodermal morphogenetic cell movements during gastrulation. *Development* 121: 877–886, 1995.
73. **Yang JT, Rayburn H, and Hynes RO.** Cell adhesion events mediated by α4-integrins are essential in placental and cardiac development. *Development* 121: 549–560, 1995.